

Inert Gases in Solids: Interatomic Potentials and Their Influence on Rare-Gas Mobility*

W. D. Wilson and C. L. Bisson
Sandia Laboratories, Livermore, California 94550
 (Received 17 February 1971)

A modification of the Wedepohl method for the determination of interatomic potentials between closed-shell atoms and ions was developed and applied to the rare gases. Both Slater and Kohn-Sham exchange approximations were employed in the calculation of the atomic charge distributions and also in the overlap region between the atoms. The He-Cu⁺ and short-range Cu⁺-Cu⁺ interactions were calculated by the same technique. Using five different potentials to describe the copper lattice, the minimum energy configuration of an interstitial He atom was determined. The (1,0,0) octahedral position in the lattice was found to be most stable, independent of the potential. Despite the variations in the potentials, the activation energy for He migration was found to lie within the narrow range 0.45 to 0.71 eV and the path of migration was found to be along a $\langle 110 \rangle$ crystallographic direction. Our calculations therefore show that interstitial He atoms will be mobile at or below room temperature in a trap-free copper lattice.

I. INTRODUCTION

By far the majority of theoretical investigations of the characteristics of inert gases in crystals have been confined to macroscopic considerations.¹ Notable exceptions are the early work of Rimmer and Cottrell² on inert gases in metals; the calculations of Anderman and Gehman³ on Xe in Cu; studies by Norgett and Lidiard⁴ on Ar and Kr migration in potassium and rubidium halides; and the more recent calculations by Dellin *et al.*,⁵ Wilson and Johnson,⁶ Harrison and Fischer,⁷ and Jaswal and Striefler⁸ on He in LiH. These calculations are atomistic in nature, and as such require a detailed knowledge of the interatomic potentials involved over a wide range of internuclear separations. The accuracy of these calculations is therefore limited by the approximations used for these potentials.

In the case of LiH, there are few enough electrons to treat the problem from a "first-principles" point of view; that is, interatomic potentials for Li⁺-H⁻, H⁻-H⁻, Li⁺-Li⁺, He-H⁻, and He-Li⁺ could be obtained using molecular-orbital theory,^{8,9} and then a polarizable and perhaps also deformable⁸ point-ion calculation performed to obtain the He migration energies. Harrison and Fischer⁷ calculated the activation energy for He migration in LiH completely quantum mechanically, and this perhaps represents the most basic defect calculation performed to date. It is encouraging that the range of activation energies is so narrow (0.60 eV,⁵ 0.69 eV,⁶ 0.54 eV,⁷ 0.65 eV⁸) considering the differences in the models and calculational techniques employed.

For many-electron systems, host-atom potentials are usually fitted to available experimental crystal data and then some appropriate approxima-

tion made to the rare-gas-lattice-atom interaction. Rimmer and Cottrell² averaged the Cu-Cu and He-He potentials to obtain the He-Cu interaction; Norgett and Lidiard used the mean of the K⁺ and Cl⁻ radii as the Ar radius in the generalized Huggins-Mayer form to obtain their Ar-K⁺ and Ar-Cl⁻ interactions. Since the host-atom potentials themselves are known only about the interionic separation (having been fitted to crystal data) the use of these potentials in cases where relaxations of lattice atoms are appreciable can lead to errors which are difficult to estimate.

The present work is concerned with the development of a technique for obtaining pairwise interatomic potentials for closed-shell atoms and ions for use in defect studies. Because of the great deal of experimental and theoretical effort which has already been devoted to the study of rare gases, these systems form a convenient starting point for our investigations.

Over the past three decades, Amdur and co-workers^{10,11} have studied rare-gas interactions using molecular beam scattering techniques. This method gives detailed information about the potential over a limited range of interatomic separations, depending upon the energy of the beam particles. Their studies have, to date, yielded accurate potentials for homonuclear systems¹⁰ (excluding radon) and a few heteronuclear cases such as He-Ar and Ne-Ar.¹¹ Kamnev and Leonas¹² have also used scattering techniques to determine He-He, Ne-Ne, Ar-Ar, He-Ar, He-Ne, and Ne-Ar potentials over internuclear distances of 0.87–3.14 Å, depending upon the system studied. High-temperature diffusion measurements of the He-Ar system have been performed by Walker and Westenberg¹³ in the 2.21–2.57 Å range of interatomic separations. In these ranges the attractive part

of the potential is negligible, that is, both scattering and high-temperature diffusion measurements study the repulsive portion of the potential energy curve between rare gases.

Several theoretical papers on rare gases have also appeared. Phillipson¹⁴ has performed a single-configuration molecular-orbital calculation of the He-He repulsive interaction. Matcha and Nesbet¹⁵ have calculated He-Ne, He-Ar, and Ne-Ar repulsive potentials in the molecular Hartree-Fock approximation. Gilbert and Wahl¹⁶ have calculated He-He, Ne-Ne, and Ar-Ar potentials, also using the complete self-consistent-field (SCF) approach. Although these calculations represent the best first-principles treatment of inert gas interactions, the effort involved in their determination can be prohibitive except for the simplest cases (such as LiH mentioned above). For example, Gilbert and Wahl point out that a single SCF calculation on Ne-Ne required 80 min on an IBM 7094 without optimizing the exponents in their wave functions. It is clear that approximate methods must be sought which will make possible the calculation of interatomic potentials for a wide variety of atoms and ions.

The Thomas-Fermi model of Firsov¹⁷ represents an early attempt at such an approximation. Abrahamson, Hatcher, and Vineyard¹⁸ included exchange effects in the free-electron approximation to establish the Thomas-Fermi-Dirac (TFD) approximation. Subsequent calculations by Abrahamson¹⁹ are to our knowledge the most complete set of rare-gas interactions. Recently, Abrahamson used the TFD approximation to determine potentials between all *neutral atoms* from atomic number $Z = 2$ to $Z = 105$.²⁰ One of the shortcomings of the method is that the charge distributions do not exhibit the quantum-mechanical shell structure known to exist, and therefore the effect of this structure on the interactions cannot be determined. Another problem is that the distributions have an arbitrary cutoff "radius" beyond which they abruptly drop to zero. The method is quite rapid, however, and the results are in reasonable agreement with experiment.

Another approximate procedure, the one we shall most closely follow here, is due to Wedepohl.²¹ In this method, the interaction between two charge distributions and nuclei is classically determined and the increase in kinetic and exchange energies in the overlap region included as a correction in the Slater free-electron approximation.²² Because the purpose of Wedepohl's work was to determine the influence of the charge distributions of atoms and ions on the interatomic potentials, no attempt was made to calculate these distributions—existing SCF and TFD densities were employed. Furthermore, several of the necessary integrals were evaluated numerically, although they could have

been reduced to analytic form.

In Sec. II, a brief discussion of the modified Wedepohl method is given and the technique applied to the determination of the repulsive region of all pairwise rare-gas potentials. The effect of exchange and "tail-corrections" are also discussed in Sec. II and the He-Cu⁺ potentials needed for the defect calculations presented. Section III contains the required host-atom potentials and in Sec. IV the results of our calculations of interstitial rare-gas configurations and activation energies for motion of these atoms are presented. The effect of using various potentials in the defect calculation is also discussed in Sec. IV.

II. RARE-GAS INTERACTIONS

As mentioned earlier, the present work is a modification of the Wedepohl²¹ method. Wave functions and, hence, charge distributions were determined using the Herman-Skillman program²³ which employs the Slater²² approximation to the exchange. A similar method has been independently developed by Harrison.²⁴ We write the total energy of interaction between two charge distributions as the sum of the electron-electron E_{ee} ; electron-nuclear E_{en} ; nuclear-nuclear E_{nn} ; kinetic E_k ; and exchange energy E_a :

$$E = E_{ee} + E_{en} + E_{nn} + E_k + E_a .$$

The last two terms are evaluated in the overlap region only. The electrostatic interaction between the two spherical charge distributions, E_{ee} , is determined by dividing the distributions into elementary spherical shells and then obtaining the interaction between these shells classically. Unlike Wedepohl, the integration over r , the distance between the shell centers or nuclei, was done analytically to eliminate an unnecessary logarithmic interpolation scheme and possible numerical inaccuracy. Also, the distributions were not cut off at some arbitrary radius but the complete set of Hartree-Fock-Slater radial wave functions were used to determine the distributions. In all the numerical work we used the Herman-Skillman 441 point integration mesh and a six-point Newton-Cotes integration procedure. Gauss's law considerations were employed in the calculation of the electron-nuclear E_{en} term—again to eliminate the integration over r . The nuclear-nuclear term is, of course, straightforward. The kinetic and exchange terms were calculated by first transforming the coordinate system into one which allows direct integration over the Herman-Skillman mesh—a procedure outlined by Abrahamson.¹⁹ Wedepohl used a 61 point mesh for this calculation and a different coordinate system but we found the E_k and E_a terms to be a very slowly converging function of this grid size.

With respect to the exchange term; much interest

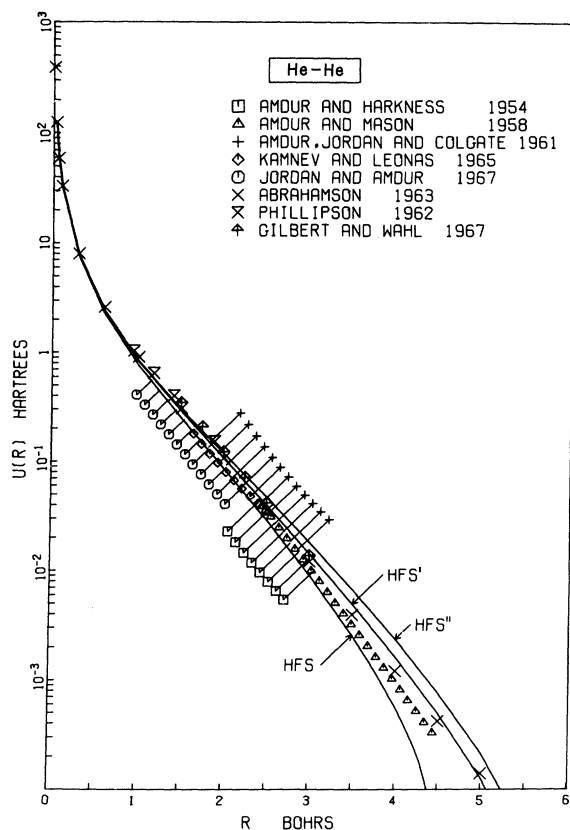


FIG. 1. He-He interatomic potentials. The three solid lines are the present results (see text for definitions of HFS, HFS', and HFS''). The first five references in the legend refer to experimental results and the remaining three to theoretical work.

has recently arisen from a suggestion by Gaspar²⁵ and Kohn and Sham²⁶ that the Slater approximation to the exchange overestimates the effect by a factor of $\frac{3}{2}$. In a recent paper by Slater, Wilson, and Wood,²⁷ five different approximations to the exchange were compared with the Hartree-Fock method for the Cu^+ ion. It was found that the " $X\alpha$ " method, which consists of multiplying the Slater expression by α , gave nearly as good results for the energy of the atom for a value of $\alpha = 0.77$ as a much more complicated method of using different exchange potentials for each orbital. In an examination of exchange approximations for neutral argon, Cowan *et al.*²⁸ concluded that the orbitals determined using the Kohn-Sham exchange ($\alpha = \frac{2}{3}$) gave the best agreement with the Hartree-Fock orbitals but that the Slater ($\alpha = 1$) exchange gave the best one-electron energies. Following a suggestion made by Sham, Cowan *et al.*²⁸ also investigated the effect of excluding the "tail correction" on the eigenvalues and eigenfunctions of Ar. Their results show that a significant improvement in the one-electron wave functions can result if this

correction is eliminated. We therefore investigated the effect of using different exchange terms and were careful to employ the same approximation in the atomic and diatomic calculations.

In Figs. 1-6, the results of our calculations of rare-gas pairwise potentials are given and compared with results of other workers. Since we are interested only in the repulsive portion of the curves, data such as that determined from low-temperature diffusion measurements was not included. We have also avoided plotting the repulsive portions of various fits to potentials (such as exponential-6) because of the uncertainty in their range of validity. The three solid lines in each figure are our theoretical results for each of three approximations used. The notation is as follows. HFS: Slater exchange including tail correction; HFS'': Kohn-Sham exchange including tail correction; HFS': Kohn-Sham exchange excluding tail correction. (In an unpublished report,²⁹ we calculated the one-electron eigenvalues and expectation values of r , $\langle r \rangle$, for each of the rare-gas atoms and compared them to the Hartree-Fock calculations of Nestor *et al.*³⁰ It was

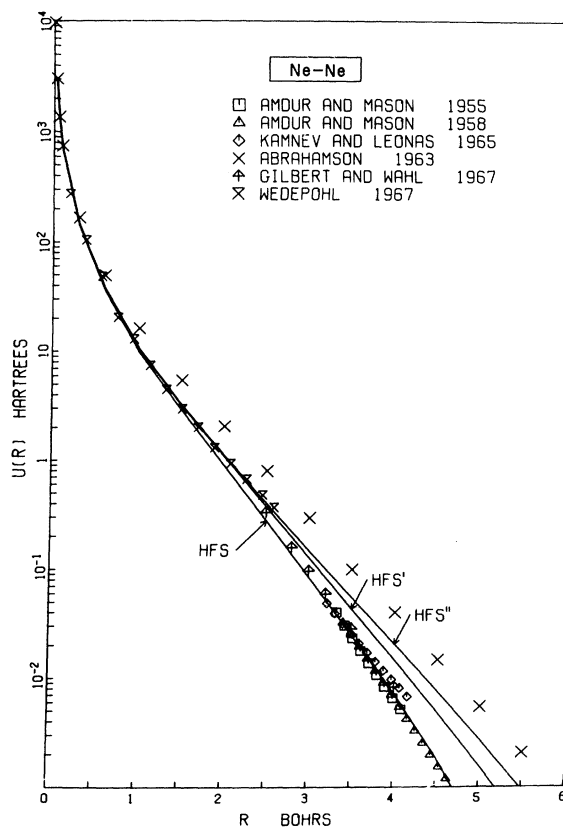


FIG. 2. Ne-Ne interatomic potentials. The three solid lines are the present results (see text for definitions of HFS, HFS', and HFS''). The first three references in the legend refer to experimental results and the remaining three to theoretical work.

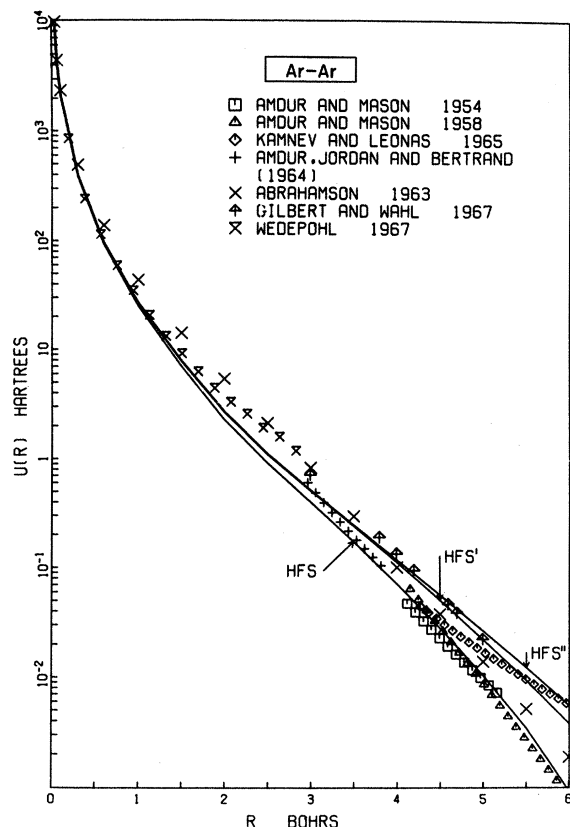


FIG. 3. Ar-Ar interatomic potentials. The three solid lines are the present results (see text for definitions of HFS, HFS', and HFS''). The first four references in the legend refer to experimental results and the remaining three to theoretical work.

found that for Ne, Ar, Kr, and Xe the $\langle r \rangle$ for the outermost orbital was best in the HFS' approximation—consistent with the results of Cowan *et al.*²⁸ For Ar, Kr, and Xe, the HFS'' gives the best *overall* one-electron functions, whereas for He, the HFS or Slater approximation to the exchange was closest to the Hartree-Fock values. In all cases, the one-electron eigenvalues were best in the HFS approximation.)

There are some general features of all the curves (Figs. 1–6) that are to be noted. Over several orders of magnitude in the energy, for intermediate values of internuclear separation, the curves are very nearly straight lines on a semilog scale, that is, Born-Mayer behavior obtains for a large portion of each curve. At smaller separations there is a rapid deviation from this behavior, energy varying as $1/r$, where r is the internuclear separation. This is the familiar Bohr dependence on distance which occurs because of the dominance of the nuclear-nuclear interaction at small separations. At large separations, particularly for the HFS approx-

imation, there is a tendency for the energy to become negative. Although not shown in the figures, these negative values actually exhibit "well-like" behavior with depth of the order of 0.001 eV, much like a weakly bound state of the diatomic system. These negative minima are consistent with the classical behavior to be expected from the method as discussed by Wedepohl.²¹ We do not attribute any real physical significance to these minima because of the approximations used but recognize the possibility of the existence of weakly bound states of this order in such interactions.^{31,32}

In Figs. 1–6, the HFS curve lies lowest and the HFS'' curve highest in energy, consistent with the magnitude of the (negative) exchange included in each of these approximations. The difference between the HFS and HFS'' curves increases with separation becoming as much as an order of magnitude in energy. Since the total energy of interaction is given by a sum of positive and negative terms, the numerical accuracy of the calculation decreases with increasing separation. Unfortunately, this is also true of the Hartree-Fock calcula-

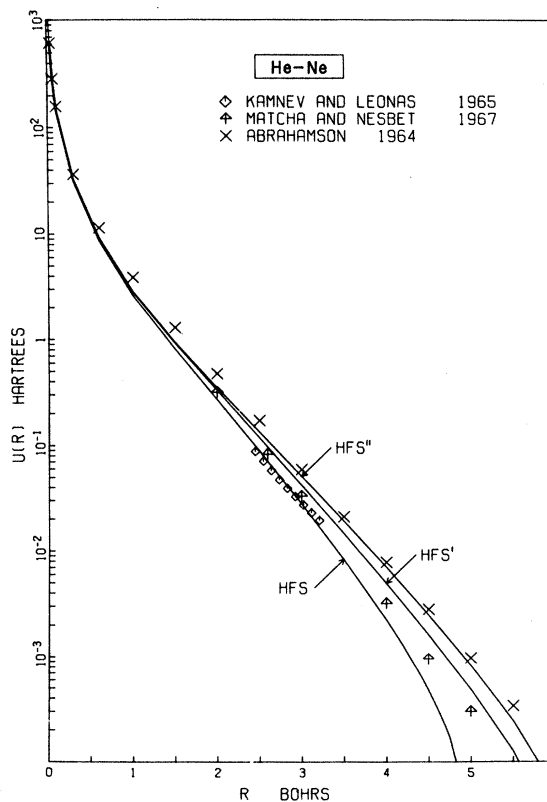


FIG. 4. He-Ne interatomic potentials. The three solid lines are the present results (see text for definitions of HFS, HFS', and HFS''). The first reference in the legend refers to experimental work and the remaining two to theoretical results.

tions, which was pointed out by Matcha and Nesbet¹⁵ (and also by Ritchie³³), making comparison with an exact value difficult. There is a smaller difference between the HFS' and HFS'' results, indicating that the tail correction is less important than the exchange approximation.

For all six rare-gas potential energy curves (Figs. 1-6), a good agreement with experiment is obtained using the HFS approximation, and the HFS' case gives the closest agreement with molecular-orbital theory. For example, the He-Ar potential curve (Fig. 6) calculated in the HFS approximation is in excellent agreement with the experimental results of Colgate *et al.*¹¹ and also Amdur *et al.*¹¹ (The experimental results of Kamnev and Leonas¹² consistently indicate a different slope from that determined by other workers, both experimental and theoretical, and hence may be attributed to some experimental difficulty.) On the other hand, the HFS' curve for He-Ar agrees quite well with the values calculated by Matcha and Nesbet.¹⁵ These authors ascribe the disagreement between molecu-

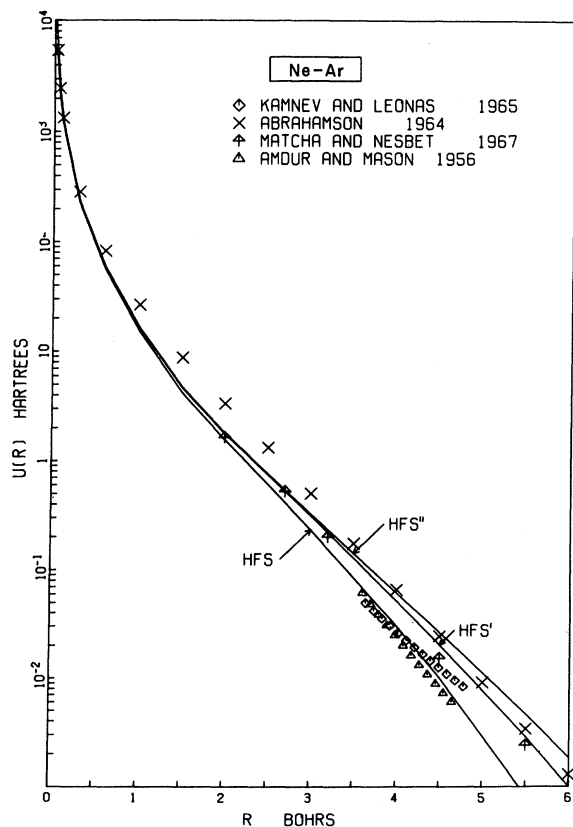


FIG. 5. Ne-Ar interatomic potentials. The three solid lines are the present results (see text for definitions of HFS, HFS', and HFS''). The first and last references in the legend refer to experimental work and the others to theoretical results.

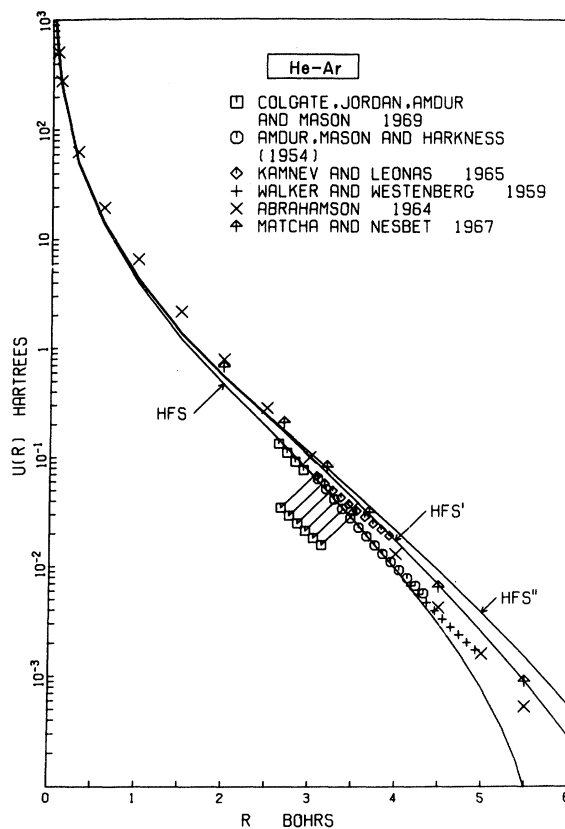


FIG. 6. He-Ar interatomic potentials. The three solid lines are the present results (see text for definitions of HFS, HFS', and HFS''). The first four references in the legend refer to experimental work and the last two to theoretical results.

lar-orbital theory and experiment to correlation effects. Our results are consistent with the interpretation that the HFS' approximation, being best for the atomic wave functions,^{28,29} also gives results for diatomic interactions in closest agreement with molecular Hartree-Fock theory. The HFS approximation, in overestimating the exchange, has in some way corrected for the higher energies obtained in this approximation and are consistently, for all rare gases, in excellent agreement with experiment. Because of the difficulties involved, we do not know if the HFS' approximation would be improved by a proper inclusion of correlation effects.

It should be noted that Wedepohl's results, shown in Figs. 2 and 3, were obtained using different charge distributions from those employed here, making only a rough comparison possible.

Based on the results shown in Figs. 1-6, the HFS'' approximation is clearly the poorest, giving interaction curves which are always even higher than the molecular-orbital theory or HFS' results. In the He-Cu⁺ and Cu⁺-Cu⁺ interactions needed for the defect calculations, therefore, we have rejected the

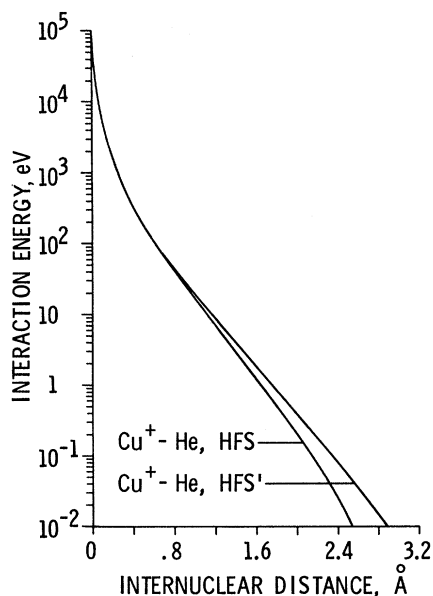


FIG. 7. Cu^+ -He interatomic potentials employed in the defect calculations (see text for definitions of HFS and HFS').

use of the HFS'' approximation. Because of its demonstrated agreement with experiment on rare gases, the HFS approximation is considered to be the best, but the HFS' is included for comparison. In Fig. 7, the He- Cu^+ interaction is plotted in the HFS and HFS' approximations. These curves display the same general features as the rare-gas potentials but no experimental data is available for comparison.

III. HOST-ATOM POTENTIALS FOR COPPER

Considerable experimental and theoretical work has been done on copper. Phonon dispersion curves,³⁴ elastic constants,³⁵ the single-vacancy formation energy,³⁶ and the threshold energy for dis-

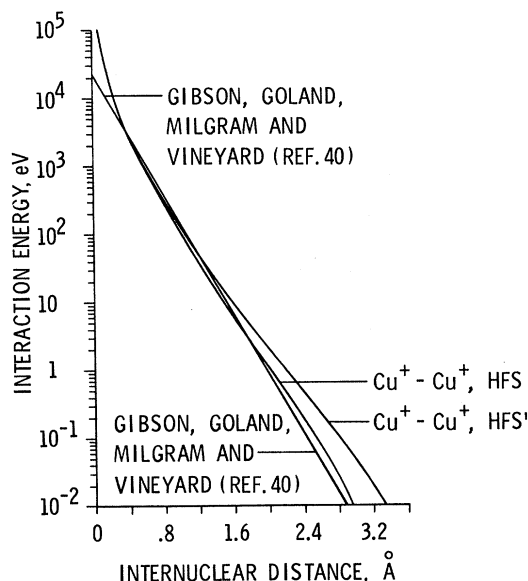


FIG. 8. Short-range Cu^+ - Cu^+ interatomic potentials used in the defect calculations (see text for definitions of HFS and HFS'). Note the agreement between the Gibson *et al.* potential and the *ab initio* HFS results of this work.

placement of a lattice atom³⁷ are quite well known for this material. Moreover, neutron irradiation and ion implantation studies of the formation and agglomeration of inert gas atoms in copper have been performed. This great wealth of information makes the calculation of the characteristics of inert gases in copper an obvious first step.

Several workers have developed potentials for the copper lattice. Huntington³⁸ used a Born-Mayer potential to study self-interstitial migration, Giral-falco and Weizer³⁹ used a Morse potential to obtain the strains produced by vacancies, and Gibson *et al.*⁴⁰ used a Born-Mayer potential to study the dynamics of radiation-damaged events. The Gibson

TABLE I. Cu-Cu interatomic potentials employed in the He interstitial calculations. Potentials I-IV are fifth-power polynomials for $r_n < r < r_c$; potential V has cubic form. In all cases, $V(r_c) = V'(r_c) = 0$; r_1 is the nearest-neighbor distance.

	Cu-Cu interatomic potential				
	I	II	III	IV	V
r_n (Å)	1.70	1.50	1.70	1.50	1.97
$V'(r_1)$, $V''(r_1)$	Elastic constants	Phonon dispersion curves	Phonon dispersion curves	Phonon dispersion curves	Elastic constants
$V(r \leq r_n)$, $V'(r_n)$ taken from:	Reference 40	Fig. 8 (HFS)	Fig. 8 (HFS)	Fig. 8 (HFS')	Reference 40
He- Cu^+ potential	Fig. 7 (HFS)	Fig. 7 (HFS)	Fig. 7 (HFS)	Fig. 7 (HFS')	Fig. 7 (HFS)

*et al.*⁴⁰ potential was chosen because it gave reasonable agreement with the threshold energy for displacement of a Cu atom. Recent work by Anderman⁴¹ and by Johnson⁴² employed potentials which were fitted to this Born-Mayer form at some small separation r_n . Anderman used a composite cubic potential at intermediate separations having cutoff between first and second nearest neighbors, the parameters in which were fitted to the elastic constants. This was done because of Johnson's earlier success with such a potential for iron and nickel.⁴³

Johnson⁴² has recently suggested a fifth-power potential for copper at separations greater than some arbitrary r_n , with the Gibson *et al.*⁴⁰ potential again used for smaller internuclear distances. The value $V(r_n)$ and first derivative $V'(r_n)$ of this potential are fitted to the Gibson *et al.* potential; the value $V(r_1)$ (where r_1 is the first-nearest-neighbor distance) is fitted to the vacancy formation energy [$V(r_1) = -0.2$ eV]; $V'(r_1)$ and $V''(r_1)$ are given by either the elastic constants or phonon dispersion curves; and the value $V(r_c)$ and first derivative $V'(r_c)$ are set to zero at a cutoff radius r_c which is determined by the choice of r_n . In this way, the potential is constructed with one adjustable parameter r_n , which Johnson varied within reasonable limits in his calculation of interstitials and vacancies in copper. This model, however simple, gives excellent agreement with the phonon dispersion curves for Cu over the entire Brillouin zone.

Our choices of potentials are similar to Johnson's in that the same functional form and general conditions are employed. The short-range potential, however, was determined by the Wedepohl method in the HFS and HFS' approximations. In Fig. 8, a comparison of these potentials with the empirical Gibson *et al.*⁴⁰ potential is given. Again, the HFS approximation agrees closely with the empirical potential which was fitted to the experimental crystal data. The HFS' approximation lies higher than the empirical results would indicate (as it did for the rare gases) but is included for comparison purposes.

We have employed five Cu-Cu potentials in our defect calculations. Potential I is Johnson's potential⁴²

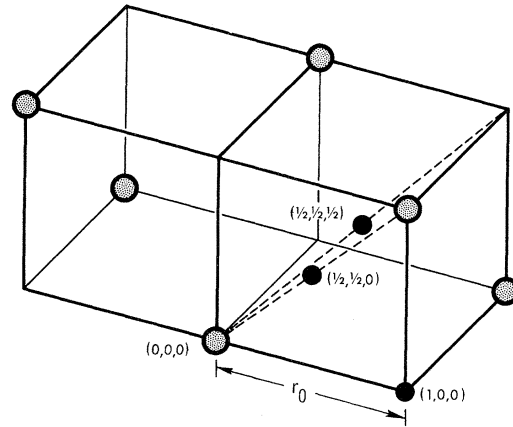


FIG. 9. Possible interstitial positions of an inert gas atom in an fcc lattice. The small solid spheres represent He atoms and the larger spheres Cu atoms.

for $r_n = 1.70$ Å (fitted to the elastic constants and the Gibson *et al.*⁴⁰ short-range form). Potential II is a modification of this potential which is fitted to the Cu⁺-Cu⁺ (HFS) potential given in Fig. 8 at a value of $r_n = 1.50$ Å and also to the full phonon dispersion curves rather than the long-wavelength limit only (elastic constants). Potential III is the same as II except that here $r_n = 1.70$ Å; potential IV is the same as II with the exception of using the HFS' instead of the HFS Cu⁺-Cu⁺ potential. Anderman's cubic potential⁴¹ was taken as potential V. The choice of potentials II-IV will enable us at least to determine the sensitivity of our results to the value of r_n and to the HFS or HFS' approximations. Potentials I and V were chosen specifically because of their previous use in the calculations of Johnson and Anderman. The above descriptions of the potentials are summarized in Table I.

As a check on our method, we calculated the vacancy formation energy E_{1V}^F for all five potentials (I-V). Johnson's⁴² potential I gave $E_{1V}^F = 1.19$ eV with 458 atoms allowed to relax, in excellent agreement with Johnson's calculation of $E_{1V}^F = 1.17$ eV. The small difference can be ascribed to the larger

TABLE II. Displacement parameters p_1 assigned to first nearest neighbors in each of the interstitial rare-gas configurations.

First-nearest-neighbor coordinates	Rare gas at (1, 0, 0)	Rare gas at ($\frac{1}{2}, \frac{1}{2}, 0$)	Rare gas at ($\frac{1}{2}, \frac{1}{2}, \frac{1}{2}$)
0, 0, 0	$-p_1, 0, 0$	$-p_1, -p_1, 0$	$-p_1, -p_1, -p_1$
1, 1, 0	$0, p_1, 0$	$p_1, p_1, 0$	$p_1, p_1, -p_1$
1, -1, 0	$0, -p_1, 0$		
1, 0, -1	$0, 0, -p_1$		
1, 0, 1	$0, 0, p_1$		$p_1, -p_1, p_1$
2, 0, 0	$p_1, 0, 0$		
0, 1, 1			$-p_1, p_1, p_1$

TABLE III. Formation energies E^F in eV and first-nearest-neighbor displacement parameters p_1 for a He interstitial atom in a (1, 0, 0), $(\frac{1}{2}, \frac{1}{2}, 0)$, and $(\frac{1}{2}, \frac{1}{2}, \frac{1}{2})$ position (in units of the half-lattice constant) in a copper lattice. The values of p_1 are given in parenthesis.

Potential employed	He interstitial position			Activation energy (eV)
	(1, 0, 0)	$(\frac{1}{2}, \frac{1}{2}, 0)$	$(\frac{1}{2}, \frac{1}{2}, \frac{1}{2})$	
I	1.99 (0.075)	2.61 (0.203)	2.95 (0.076)	0.62
II	2.10 (0.065)	2.81 (0.196)	3.17 (0.070)	0.71
III	1.97 (0.083)	2.42 (0.222)	2.75 (0.085)	0.45
IV	3.22 (0.104)	3.76 (0.234)	4.16 (0.094)	0.54
V	1.74 (0.081)	2.23 (0.222)	2.86 (0.073)	0.49

number of atoms (530) and the inclusion of an isotropic elastic continuum by Johnson, each of which tend to lower the formation energy. Potentials II–IV also gave $E_{IV}^F = 1.19$ eV, primarily because of the fitting of these potentials to the same value, $V(r_1) = -0.2$ eV, as in potential I. Potential V gave $E_{IV}^F = 1.04$ eV in good agreement with the 0.988 eV value calculated by Anderman.⁴¹ Our calculated relaxations were also in agreement with Johnson and Anderman.

IV. INTERSTITIAL RARE-GAS CONFIGURATIONS

In this section, we describe the results of our calculations of He interstitial configurations in Cu using the potentials I–V derived above. The He–Cu⁺ potential used was the HFS shown in Fig. 7 for all except potential IV, where the HFS' approximation was used to be consistent with the Cu⁺–Cu⁺ choice. The total energy relative to the perfect Cu lattice is expressed as a function of the displacement parameters assigned to the host atoms surrounding the rare-gas impurity. This energy is then minimized with respect to each of these parameters in an iterative fashion. To lower the computer time, the $3n$ degrees of freedom (where n is the number of relaxed atoms) were reduced by making use of the symmetry of each configuration. Many authors include an elastic continuum which is added to the relaxed region of atoms. Such techniques, however, do not take into account the anisotropy of the relaxations and are therefore quite approximate. Besides, if enough atoms are allowed to displace, the effects of the continuum can be made quite small. We, therefore, performed several of our calculations with an increased number of relaxed atoms to determine the effect of neglecting the elastic continuum.

In Fig. 9, the three primary He interstitial configurations (1, 0, 0), $(\frac{1}{2}, \frac{1}{2}, 0)$, and $(\frac{1}{2}, \frac{1}{2}, \frac{1}{2})$ in units of the half-lattice constant r_0 are shown. From a knowledge of the formation energy of each of these configurations the path and activation energy for migration of rare-gas atoms can be determined.

In Table II, the displacement parameters assigned to the first nearest neighbors to the He atom in each of the symmetrical configurations are given. Table III gives the results of our calculations of the formation energy of a single He atom in each of the configurations shown for all five potentials. The number of atoms allowed to relax about the defect was kept nearly equal in each case, being 236, 232, and 228 for the (1, 0, 0), $(\frac{1}{2}, \frac{1}{2}, 0)$, and $(\frac{1}{2}, \frac{1}{2}, \frac{1}{2})$ positions, respectively. To conserve space, only the first-nearest-neighbor displacements are given in Table III.

It is first of all clear from Table III that the formation energy of a particular configuration can be significantly affected by the choice of potential. We have already shown that the HFS' approximation gave energies much higher than experiment for all rare gases and also for Cu⁺–Cu⁺. It is therefore not surprising that potential IV, which uses this approximation, gives the highest formation energies. We included this potential for comparison, however, and were encouraged that it gave rise to an activation energy of 0.54 eV, which is within the range predicted by the other potentials. In general, the greatest differences in formation energies were obtained in the $(\frac{1}{2}, \frac{1}{2}, 0)$ configuration. This is due to the closer packing and hence larger relaxations (see p_1 values in Table III) for this case which necessitates knowing the interatomic potential at distances farther from the perfect lattice distances. A comparison of potentials II and III indicates that larger matching radii lead to lower formation energies. This seems to be the general trend because the larger r_n results in a potential which is more negative over a larger region of internuclear separation.

Despite the many differences in the potentials, the (1, 0, 0) configuration consistently lies the lowest in energy with the $(\frac{1}{2}, \frac{1}{2}, 0)$ and $(\frac{1}{2}, \frac{1}{2}, \frac{1}{2})$ lying, respectively, higher. The mechanism of diffusion is therefore clearly established to be along a $\langle 110 \rangle$ direction in the Cu lattice. Furthermore, the activation energy for this motion is determined to lie in the 0.45–0.71-eV range. A He atom in Cu will therefore be mobile at or somewhat below room temperature.

In order to ensure that the saddle point for interstitial migration of the He atom is indeed the $(\frac{1}{2}, \frac{1}{2}, 0)$ position, we performed several additional calculations. The He atom was fixed at the (0.4, 0.4, 0), (0.6, 0.4, 0), (0.5, 0.4, 0) positions and the minimum energies for these configurations were determined to be 2.54, 2.42, and 2.45 eV, respectively. This indicates that there is no lower energy path than (1, 0, 0) to $(\frac{1}{2}, \frac{1}{2}, 0)$ in the $z = 0$ plane. Similarly, motion out of the plane was checked by fixing the He atom at (0.4, 0.4, 0.1), (0.6, 0.4, 0.1), (0.5, 0.4, 0.1), and (0.5, 0.5, 0.1) with the resulting

energies 2.56, 2.44, 2.47, and 2.45 eV, respectively. All these calculations were done using po-

tential III which gives 2.42 eV for the (0.5, 0.5, 0) position.

*Work supported by the U. S. Atomic Energy Commission.

- ¹F. A. Nichols, J. Nucl. Mater. 30, 143 (1969).
- ²D. E. Rimmer and A. H. Cottrell, Phil. Mag. 2, 1345 (1957).
- ³A. Anderman and W. G. Gehman, Phys. Status Solidi 30, 283 (1968).
- ⁴M. J. Norgett and A. B. Lidiard, Phil. Mag. 18, 1193 (1968).
- ⁵T. A. Dellin, G. J. Dienes, C. R. Fischer, R. D. Hatcher, and W. D. Wilson, Phys. Rev. B 1, 1745 (1970).
- ⁶W. D. Wilson and R. A. Johnson, Phys. Rev. B 1, 3510 (1970).
- ⁷S. W. Harrison and C. R. Fischer, Bull. Am. Phys. Soc. 14, 612 (1969); also, S. W. Harrison, Ph.D. thesis (City University of New York, 1970) (unpublished).
- ⁸S. S. Jaswal and M. E. Striefler, Phys. Rev. B 1, 4118 (1970).
- ⁹C. R. Fischer, T. A. Dellin, S. W. Harrison, R. D. Hatcher, and W. D. Wilson, Phys. Rev. B 1, 876 (1970); see also, R. Tseng and J. R. Hardy, UCRL Report No. 13458, 1970 (unpublished).
- ¹⁰He-He: I. A. Amdur and A. L. Harkness, J. Chem. Phys. 22, 664 (1954); I. A. Amdur, J. E. Jordan, and S. O. Colgate, *ibid.* 34, 1525 (1961); Ne-Ne: I. A. Amdur and E. A. Mason, *ibid.* 23, 415 (1955); Ar-Ar: 22, 670 (1954); S. O. Colgate, J. E. Jordan, I. A. Amdur, and E. A. Mason, *ibid.* 51, 968 (1969); Kr-Kr: I. A. Amdur and E. A. Mason, *ibid.* 23, 2268 (1955); Xe-Xe: 25, 624 (1956).
- ¹¹He-Ar: I. A. Amdur, E. A. Mason, and A. L. Harkness, J. Chem. Phys. 22, 1071 (1954); S. O. Colgate, J. E. Jordan, I. A. Amdur, and E. A. Mason, *ibid.* 25, 632 (1956).
- ¹²A. B. Kamnev and V. B. Leonas, Dokl. Akad. Nauk SSSR 162, 798 (1965) [Soviet Phys. Doklady 10, 529 (1965)].
- ¹³R. E. Walker and A. A. Westenberg, J. Chem. Phys. 31, 519 (1959).
- ¹⁴P. E. Phillipson, Phys. Rev. 125, 1981 (1962).
- ¹⁵R. L. Matcha and R. K. Nesbet, Phys. Rev. 160, 72 (1967).
- ¹⁶T. L. Gilbert and A. C. Wahl, J. Chem. Phys. 47, 3425 (1967).
- ¹⁷O. B. Firsov, Zh. Eksperim. i Teor. Fiz. 32, 1464 (1957); 33, 696 (1957) [Sov. Phys. JETP 5, 1192 (1957); 6, 534 (1958)].
- ¹⁸A. A. Abrahamson, R. D. Hatcher, and G. H. Vineyard, Phys. Rev. 121, 159 (1961).
- ¹⁹A. A. Abrahamson, Phys. Rev. 123, 538 (1961); 130, 693 (1963); 133, A990 (1964).
- ²⁰A. A. Abrahamson, Phys. Rev. 178, 76 (1969).
- ²¹P. T. Wedepohl, Proc. Phys. Soc. (London) 92, 79 (1967).
- ²²J. C. Slater, Phys. Rev. 81, 385 (1951).
- ²³F. Herman and S. Skillman, *Atomic Structure Calculations* (Prentice-Hall, Englewood Cliffs, N. J., 1963).
- ²⁴D. E. Harrison, Bull. Am. Phys. Soc. 14, 315 (1969).
- ²⁵R. Gaspar, Acta Phys. Acad. Sci. Hung. 3, 263 (1964).
- ²⁶W. Kohn and L. J. Sham, Phys. Rev. 140, A1133 (1965).
- ²⁷J. C. Slater, T. M. Wilson, and J. H. Wood, Phys. Rev. 179, 28 (1969).
- ²⁸R. D. Cowan, A. C. Larson, D. Liberman, J. B. Mann, and J. Waber, Phys. Rev. 144, 5 (1966).
- ²⁹W. D. Wilson and C. Bisson, Sandia Laboratories Report No. SCL-DC-70-45, 1970 (unpublished). Also in this report the pairwise potentials for all other rare gases are given.
- ³⁰C. W. Nestor, T. C. Tucker, T. A. Carlson, L. D. Roberts, F. B. Malik, and C. Froese, Oak Ridge National Laboratory Report No. ORNL-4027 (unpublished).
- ³¹Henry F. Schaefer, III, Donald R. McLaughlin, Frank E. Harris, and Berni J. Alder, Phys. Rev. Letters 25, 988 (1970).
- ³²P. Bertocini and Arnold C. Wahl, Phys. Rev. Letters 25, 991 (1970).
- ³³A. B. Ritchie, J. Chem. Phys. 52, 2541 (1970).
- ³⁴S. K. Sinha, Phys. Rev. 143, 422 (1966).
- ³⁵W. C. Overton, Jr. and J. Gaffney, Phys. Rev. 98, 969 (1955).
- ³⁶R. O. Simmons and R. W. Balluffi, Phys. Rev. 129, 1533 (1963).
- ³⁷A. Sosin, Phys. Rev. 126, 1698 (1962).
- ³⁸H. B. Huntington, Phys. Rev. 91, 1092 (1953).
- ³⁹L. A. Girafalco and V. G. Weizer, Phys. Rev. 114, 687 (1959).
- ⁴⁰J. B. Gibson, A. N. Goland, M. Milgram, and G. H. Vineyard, Phys. Rev. 120, 1229 (1960).
- ⁴¹A. Anderman, *Atomics International Report No. AI-66-252*, 1966 (unpublished).
- ⁴²R. A. Johnson, *Radiation Effects* 2, 1 (1969).
- ⁴³R. A. Johnson, Phys. Rev. 134, A1329 (1964); 145, 423 (1966); 152, 629 (1966).